Low-noise, transformer-coupled resonant photodetector for squeezed state generation

Chaoyong Chen, Shaoping Shi, and Yaohui Zheng

Citation: Review of Scientific Instruments **88**, 103101 (2017); doi: 10.1063/1.5004418
View online: http://dx.doi.org/10.1063/1.5004418
View Table of Contents: http://aip.scitation.org/toc/rsi/88/10
Published by the American Institute of Physics

Low-noise, transformer-coupled resonant photodetector for squeezed state generation

Chaoyong Chen, Shaoping Shi, and Yaohui Zheng[a)]
State Key Laboratory of Quantum Optics and Quantum Optics Devices, Institute of Opto-Electronics, Shanxi University, Taiyuan 030006, China and Collaborative Innovation Center of Extreme Optics, Shanxi University, Taiyuan, Shanxi 030006, People's Republic of China

(Received 9 May 2017; accepted 12 September 2017; published online 2 October 2017)

In an actual setup of squeezed state generation, the stability of a squeezing factor is mainly limited by the performance of the servo-control system, which is mainly influenced by the shot noise and gain of a photodetector. We present a unique transformer-coupled *LC* resonant amplifier as a photodetector circuit to reduce the electronic noise and increase the gain of the photodetector. As a result, we obtain a low-noise, high gain photodetector with the gain of more than 1.8×10^5 V/A, and the input current noise of less than 4.7 pA/$\sqrt{\text{Hz}}$. By adjusting the parameters of the transformer, the quality factor Q of the resonant circuit is close to 100 in the frequency range of more than 100 MHz, which meets the requirement for weak power detection in the application of squeezed state generation. *Published by AIP Publishing.* https://doi.org/10.1063/1.5004418

I. INTRODUCTION

Squeezed state is a special class of minimum uncertainty states, whose uncertainty of one of the quadratures is reduced compared to a vacuum state at the expense of the perpendicular quadrature. Because of the special noise properties of the squeezed states, states with a high degree of squeezing are not only one of the most promising methods available to improve the sensitivity of laser interferometer gravitational wave detectors[1,2] but also an important resource to construct entanglement states for quantum information and quantum metrology.[3,4] A typical method to generate a squeezed state is to use a sub-threshold optical parametric oscillator (OPO).[5,6] By improving the stability of cavity locking and phase locking and reducing the system loss, high level squeezing was experimentally generated.[7] The Pound-Drever-Hall (PDH) technique is one of the most effective ways to stabilize the laser phase and frequency in the quantum optics experiment.[8,9]

In the PDH locking setup, the performance of the servo-control system directly impacts the stability of the OPO, which will cause a limitation to the squeezed degree. Small variations δL in cavity length can influence the squeezing angle and increase the optical losses, leading to a drop in the level of squeezing.[10,11] Referring to the analysis in Refs. 10 and 11, we present a numerical analysis of the influence of the OPO cavity length variation δL on the squeezing level, which is shown in Fig. 1. When the OPO cavity is on resonance, $\delta L = 0$, the squeezing level reaches the maximum. The squeezing level decreases with the increase of the OPO cavity detuning. The photodetector, as the first stage of the feedback loop, is the key of the servo-control system.

In the experiment of squeezed state generation,[12,13] in order to obtain the high squeezing level, the OPO operates on the under-coupled condition, which weakens the error signals of locking the cavity and the relative phase of seed light and pump light. Thus, there needs a low-noise, high-gain photodetector to compensate the disadvantage induced from the under-coupled cavity. In addition, in order to meet the requirements for locking the mode-cleaners, the OPO, the relative phase, and so on in the quantum optics experiment,[5–7,12–14] the photodetectors work at the different frequency points between several MHz and one hundred MHz for different locking servo systems. So it requires the photodetectors have an adjustable frequency point.

Numerous photoelectric discriminators use the transimpedance amplification (TIA) circuit as the current-to-voltage converter.[15–18] The TIA has the advantage of low input current noise. However, it cannot obtain high bandwidth and slew rate at the same time. So we choose a current-feedback operational amplifier (THS3201) as the preamplifier of the photodetector. The operational amplifier has a large bandwidth of 1.8 GHz and a high slew rate of 10 500 V/μs, which meets our requirements.

A resonant circuit can boost the gain at the resonance frequency and suppress these unwanted frequency components, which is benefit of increasing the gain of the photodetector.[19–21] In our former studies, a high gain resonant photodetector has been obtained for cavity locking and phase locking by utilizing a *LC* circuit to couple the photodiode to the load directly.[22] A quality factor Q more than 90 at the resonance frequency 58.6 MHz is experimentally observed. While we adjust the resonance frequency to other bands away from 58.6 MHz by changing the inductance, the quality factor decreases, which may come from the inductance variation, loss increase, and so on. At a lower frequency, the reduction of the Q value may come from the increase of the inductance and losses. At the higher frequency, high frequency skin effect is the main cause of Q value decrease.

a)Electronic mail: yhzheng@sxu.edu.cn

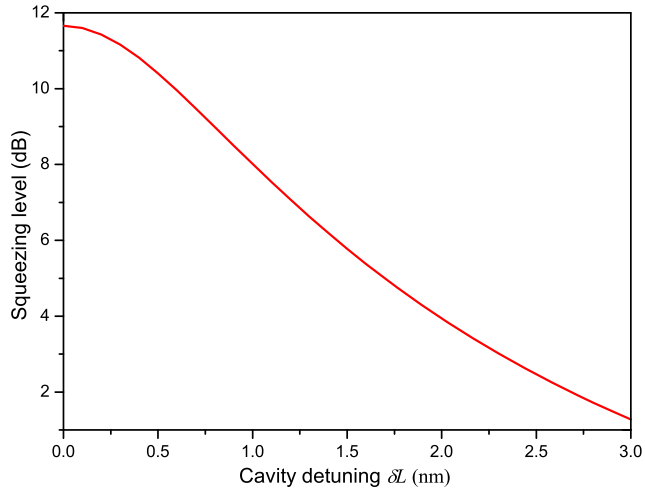

FIG. 1. Squeezing level in one quadrature of the OPO cavity output field as a function of the OPO cavity length variation δL. Here we suppose it has an ideal phase matching and the incident second harmonic pump is locked at π. With the cavity length shift increasing, the squeezing level has a sharp drop. The parameters of the OPO cavity we adopt are the normalized nonlinear coupling, $|x| = \frac{1}{\sqrt{2}}$, the escape efficiency, $\eta_{esc} = 0.96$, the cavity length on resonance, $\overline{L} = 37$ mm, the cavity field decay rate for the squeezed field, $\gamma_{s,tot} = 2\pi \times 96$ MHz, and the measurement frequency Ω which is far less than $\gamma_{s,tot}$, $\frac{\Omega}{\gamma_{s,tot}} = 1 \times 10^{-15}$.

Here we present a modified photodetector design as shown schematically in Fig. 2. We utilize a special N:1 ($N > 1$) turns ratio radio transformer to couple the photodiode to the load. The design does not only reduce the electronic noise but also increase the gain of the photodetector. A low-noise, high gain photodetector with the gain of more than 1.8×10^5 V/A and the input current noise less than 4.7 pA/$\sqrt{\text{Hz}}$ is experimentally obtained. By adjusting the parameters of the transformer, the quality factor Q of the resonant circuit is close to 100 over a frequency range of more than 100 MHz, which meets the requirement for weak power detection in the application of squeezed state generation. Compared with our previous work,[22] we analyze the noise feature of transformer-coupled resonant photodetectors, employ a multiple strands winding transformer, and obtain the resonant photodetector with a wide frequency range on the premises of keeping the quality factor Q.

II. THEORETICAL ANALYSIS

Figure 2(a) shows the schematic of the transformer-coupled resonant photodetector. The transformer-coupled resonant photodetector has three advantages over the LC-coupled resonant photodetector. First, the transformer-coupled resonant circuit can increase the equivalent transimpedance gain at the resonance frequency. Figure 2(b) gives the equivalent circuit and the noise model of the transformer-coupled photodetector. The inductance value L of the transformer primary is not random but dependent on the resonance frequency, $f = \frac{\omega_0}{2\pi} = \frac{1}{2\pi\sqrt{LC_d}}$, where C_d is the junction capacitance of the photodiode and f is the resonance frequency. This parallel resonant circuit can be considered as a current-voltage converter. The photocurrent I_p is converted into a voltage U_p dependent on the impedance Z, which is then amplified by the operational amplifier. The transfer function (frequency dependent impedance) of the parallel resonant circuit can be derived according to the principle of the circuit and RF circuit design.[24,25]

$$H(s = i\omega) = \frac{U_p}{I_p} = Z = \frac{1}{\frac{1}{sL} + sC_d + \frac{1}{R_s} + \frac{1}{R_0} + \frac{1}{N^2 R_L \beta}}. \quad (1)$$

It can be written as a typical band-pass form[26]

$$H(s) = R_\Sigma H_{BP} = R_\Sigma \frac{\frac{s}{\omega_0 Q}}{1 + \frac{s}{\omega_0 Q} + \frac{s^2}{\omega_0^2}}. \quad (2)$$

Here $\frac{1}{R_\Sigma} = \frac{1}{R_s} + \frac{1}{R_0} + \frac{1}{N^2 R_L \beta}$, R_s is the shunt resistance of the photodiode, R_0 is the loss resistance, C_d is the junction capacitance of the photodiode, and $\beta = \frac{P_{secondary}}{P_{primary}}$ is the coupling efficiency of the transformer. At the resonance frequency, the imaginary part of Eq. (1) disappears and the impedance reaches the maximum value R_Σ. At that time, the transimpedance gain G equals to GnR_Σ (Gn is the gain of the operational amplifier). Both the shunt resistance R_s and the loss resistance R_0 is far more than the load resistor R_L, and it is obvious that the turns ratio N of the transformer increases the equivalent transimpedance gain.

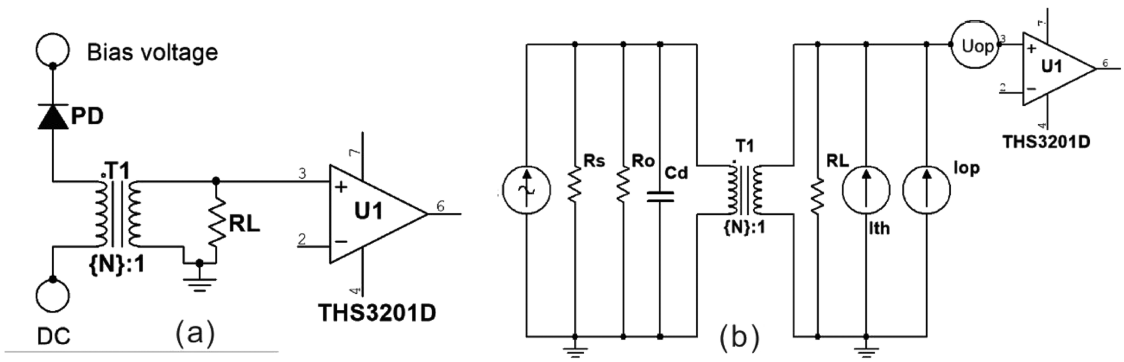

FIG. 2. (a) Schematic of the transformer-coupled resonant photodetector. Resonant circuit consists of the junction capacitance of the photodiode (C_d) and the primary of the transformer (L). The photocurrent is amplified by the N:1 turns ratio transformer and turned to voltage across the load R_L. (b) Simplified equivalent circuit and the noise model of the photodetector. R_s: the shunt resistance of the photodiode; R_0: the loss resistance; I_{th}: thermal noise in total impedance Z; I_{op}: the operational amplifier's input current noise; U_{op}: the operational amplifier's input voltage noise.

Second, the transformer-coupled resonant circuit can increase the Q value of the transfer function of the resonant circuit. The Q value is an important parameter to evaluate the resonant circuit, which is mainly determined by the load resistor R_L, the photodiode capacitance C_d, shunt resistance R_s, and the transformer (R_0, N, β). The Q value of transformer-coupled resonant circuit can be expressed as

$$Q_{tr-coupled} = \frac{R_\Sigma}{X}. \tag{3}$$

Referring to the article,[22] the Q value of the LC-coupled resonant circuit can be expressed as $Q_{LC} = \frac{R_L}{X}$, where the R_L is the load resistance and the X is the impedance of the C_d or L at the resonance frequency. Compared with the LC-coupled, if we ignore the influence of the resistances R_0, R_s, and suppose $\beta = 1$, the load resistance of the transformer-coupled resonant circuit can be simplified as N^2R_L; therefore, the quality factor $Q_{tr\text{-}coupled}$ of the transformer-coupled resonance circuit is N^2 times as large as Q_{LC} in principle. So the structure of transformer-coupled is benefit of enhancing the quality factor Q of the resonant circuit.

Surely, the Q value can also be improved by increasing the load resistor R_L. However, the R_L increase does also decrease its shunt current, further reducing the quality factor. Thus, the transformer-coupled design smartly avoids this problem. For the primary of the transformer, its equivalent load resistance is N^2 times that of R_L, which can increase the load resistance to N^2R_L. For the secondary of the transformer, the load resistor is still R_L, which does not decrease the shunt current. The value of R_L we adopted in the experiment is 8 kΩ.

Third, the transformer-coupled resonant circuit can reduce the noise equivalent current and scale up the photocurrent. The main noise sources of the photodetector are the thermal noise in total impedance Z, given by $\sqrt{4KT\Re[Z]}$, and the operational amplifier's noise (input current noise I_{op} and the input voltage noise U_{op}). To characterize the noise performance of the photodetector, it is convenient to adopt noise equivalent photocurrent I_{ne} which is defined by the condition that its shot noise contribution is the same amount of noise at the output as the rest of the circuit. Here the noise equivalent photocurrent I_{ne} (at the resonance frequency) can be given by[26]

$$I_{ne} = \frac{1}{2e}\left[\frac{4KT\Re[Z]}{|Z|^2} + \left(\frac{I_{op}}{N}\right)^2 + \frac{N^2U_{op}^2}{|Z|^2}\right]. \tag{4}$$

Here, e is the elementary charge, K is the Boltzmann constant, T is the thermodynamic temperature, $\Re[Z]$ represents the real part of the impedance Z, and the impedance Z is equal to R_Σ at the resonance frequency which can be considered to be equal to N^2R_L for simplicity. The input current noise I_{op} and the input voltage noise U_{op} of the THS3201 are 13.4 pA/$\sqrt{\text{Hz}}$ and 1.6 nV/$\sqrt{\text{Hz}}$, respectively. By simple calculation, we can know that the second term $(\frac{I_{op}}{N})^2$ plays a major role in the circuit. It is obvious that the transformer-coupled circuit can reduce the noise equivalent photocurrent. In addition, transformer-coupled circuit makes shot noise of the photocurrent dominate over the current noise from the operational amplifier.[23] Ignoring the terms of the thermal noise and the input voltage noise of the THS3201, the noise-equivalent photocurrent I_{ne} can be calculated (with turns ratio $N = 3$)

$$I_{ne} \approx 62\ \mu A. \tag{5}$$

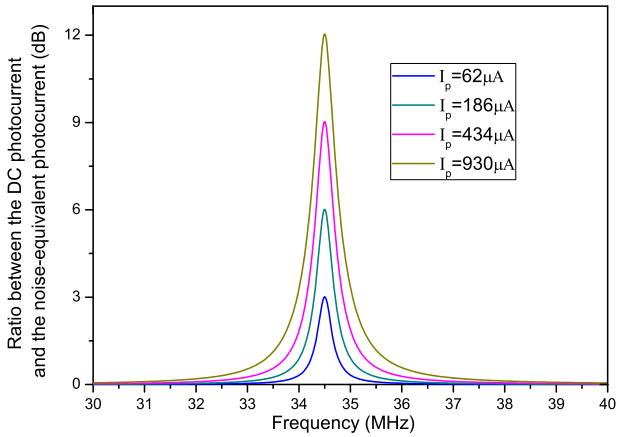

FIG. 3. Simulation of the relationship between the DC photocurrent I_p and the noise-equivalent photocurrent I_{ne}.

The shot noise limit of the photodetector can be characterized by the ratio $y(\omega)$ between the DC photocurrent I_p and the noise-equivalent photocurrent I_{ne} which is fitted with the following model:[26]

$$\begin{aligned} y(\omega) &= 20\ \log_{10}\sqrt{1 + \frac{I_p}{I_{ne}}|H_{BP}(s = i\omega)|^2}, \\ &= 10\ \log_{10}(1 + \frac{I_p}{I_{ne}}|H_{BP}(s = i\omega)|^2). \end{aligned} \tag{6}$$

Figure 3 shows the theoretical relationship between the ratio $y(\omega)$ and the DC photocurrent I_p. When the DC photocurrent I_p is $2^\alpha - 1$ (α is equal to 1, 2, 3, 4, ... in turn) times that of I_{ne}, this ratio $y(\omega)$ increases regularly 3 dB at the resonance frequency. Here the resonance frequency is set at 34.5 MHz and the Q value is equal to 120.

III. EXPERIMENTAL DESCRIPTION AND RESULTS

According to the former theoretical analysis, four points need to be considered for designing the transformer-coupled resonant photodetector. First, the inductance of the transformer primary matches with the resonance frequency, which means the number of windings is fixed for a given magnetic core. Second, the loss of the magnetic core should be as small as possible to reduce the loss resistance of the transformer. Third, the transformer should have a high coupling efficiency. Fourth, we should separate DC signal from the detected photocurrent to avoid the saturation of the AC path. In order to meet the above demands, we utilize a common core mutual coupling transformer. Its internal structure and physical map are shown in Fig. 4. The primary and the secondary of the transformer are twined in a common magnetic core. The inductance of the primary can be finely adjusted by changing the position of the core within the coil. A metal shell is used to shield the interference coming from other RF signals. In order to reduce the skin effect, the multiple strands of enameled wire

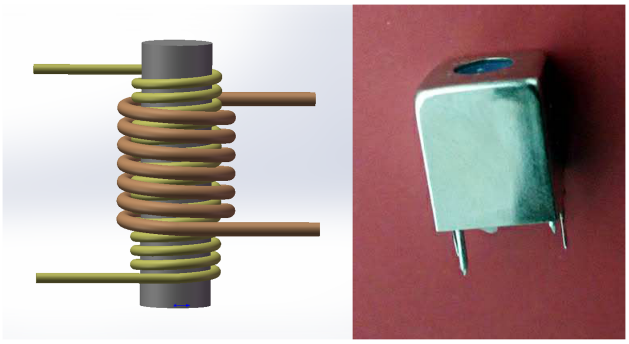

FIG. 4. The internal structure and the physical map of the transformer.

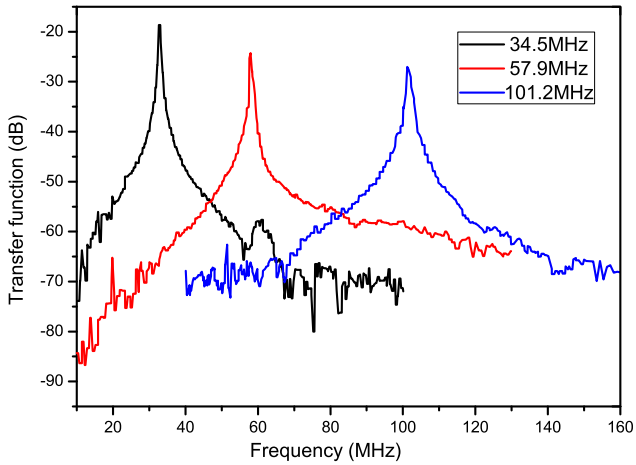

FIG. 5. The transfer functions of the transformer-coupled resonant photodetector.

are adopted. The transformer turns ratio N is a key factor of determining the Q value, which should be chosen in terms of the specific circuit. In the ideal case, the greater the turns ratio, the greater the Q value is. However, large turns ratio will reduce the coupling efficiency and also increases the loss in the practical case.

Based on the above analysis, we construct the transformers by winding the secondary coil over the commercially available coil inductors. Three commercially available coil inductors are utilized to construct three transformers for different frequency bands application, respectively. But their turn number of windings is manually adjusted as needed. An InGaAs photodiode with the model of ETX500T is adopted as the photoelectric conversion device. The ETX500T has a high quantum efficiency ($\eta \geqslant 95\%$) at 1064 nm. Its responsivity η is about 0.75 A/W at 1064 nm and its junction capacitance is 35 pF with a 5 V bias voltage. In a typical PDH setup, the beam reflected from a cavity can be considered as an amplitude modulated beam. This amplitude modulated laser beam is sensed by a photodetector and then fed into the network analyzer. The network analyzer performs a normalized measurement by calculating the ratio between the photodetector output and the internal reference signal.[22] We measured the transfer function of the transformer-coupled photodetector and the results are shown in Fig. 5. We give three representative resonance frequency points and their corresponding Q values, bandwidth, and coil turns ratio, shown in Table I. These three resonance frequency points are obtained separately by using three different transformers which are restructured by three adjustable coil inductances and suitable for different frequency regions, respectively (also shown in Table I). The resonance frequency points can be roughly adjusted by replacing the transformer or changing the turns number of the transformer primary and then be finely adjusted by changing the position of the core within the coil or adjusting the bias voltage of the photodiode. The junction capacitance of the photodiode ETX500T can be changed over ten pF by tuning the bias voltage. As a result, the resonant point can be changed about several MHz, which broadens the adjustment bandwidth of the photodetector. In this adjustment process, the quality factor Q and coupling efficiency β should to be kept in mind. Utilizing the exquisite design and fine regulation, an adjustable bandwidth more than 100 MHz with a high quality factor close to 100 can be achieved. The transimpedance gain G can be calculated by $G = GnR_{\Sigma}$ and formula (3). The $G_{(101.2\ \mathrm{MHz})} = 1.81 \times 10^5$ V/A with the $L = 160$ nH and the $Gn = 20$. The main reason for the Q value reduction at the high resonance frequency is the decrease of the transformer coupling efficiency and the increase of the coil loss. It may be improved if better transformer material is used. We employ multiple strands of enameled wire to decrease of the coil loss in the experiment.

Another parameter that we focused on is the tunability of the transformer-coupled detector. Figure 6 shows the tunability of one detector. First we measured the peaks of the transfer function (magenta trace) and the Q values (green trace) for different resonance frequencies by changing the core position only. With the magnetic core away from the center of the coil, the inductance value L decreases and the resonance frequency increases. When the magnetic core is away from the center of the coil, both the peak values and the Q values decrease, which do mainly originate from the decrease of the coupling efficiency. The above results also show the

TABLE I. The resonance frequency points and the corresponding Q value, bandwidth, and coil turns ratio.

Resonant frequency (MHz)	Q value	BW (MHz)	Coil turns ratio	The inductances adopted	Applicable frequency range (MHz)
34.5	126	0.26	3:1	No model number[a]	1–50
57.9	111	0.52	2:1	E526HN-100109[b]	30–80
101.2	89	1.14	5:3	E526HNA-100314[c]	70–120

[a]A low loss high frequency inductors without model number.
[b]Toko America, Inc. Model number: E526HN-100109.
[c]Toko America, Inc. Model number: E526HNA-100314.

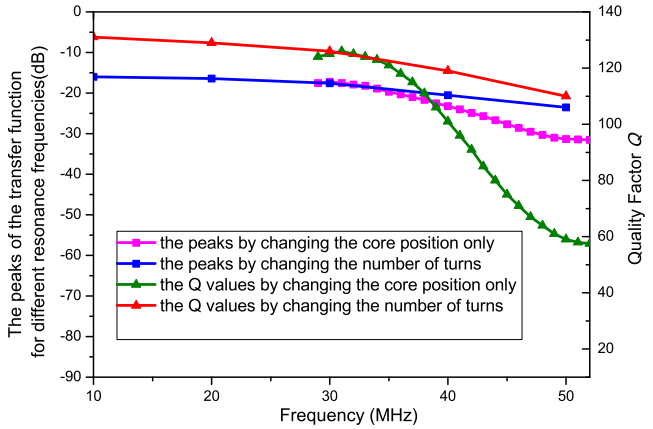

FIG. 6. The tunability of one of the transformer-coupled detectors. The magenta and green trace give the peaks of the transfer function and the Q values for different resonance frequencies by changing the core position only. The blue and red traces are obtained by changing the number of turns of the transformer coil and the position of the core (close to the center of the coil), which gives the peaks of the transfer function and the Q values for different frequency points, respectively.

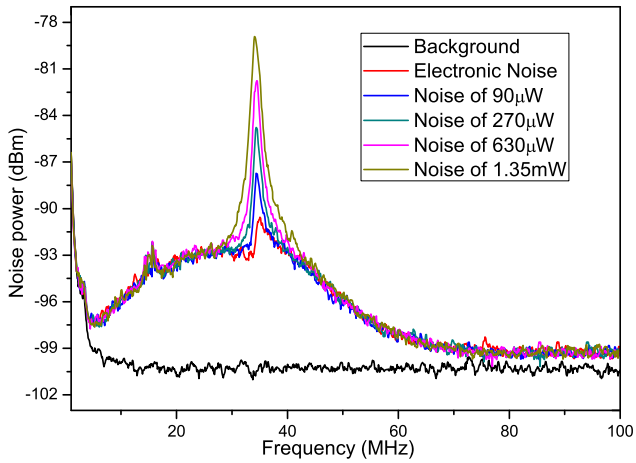

FIG. 7. Noise power measurement of different laser power without modulation. It is measured by the spectrum analyzer (Agilent, N9020A), with RBW = 51 KHz, VBW = 51 Hz, and seep time = 1 s.

trend of the transformer coupling efficiency as the resonance frequency changes. Subsequently, we kept the magnetic core in the center of the coil and changed the number of turns of the transformer coil. The blue and red traces in Fig. 6 show that the peaks of the transfer function and the Q values vary with the resonant frequency, which are relevant to the number of turns of the transformer coil. Both the peaks and the Q values have a small drop with the increase of the resonance frequency. Comparing with adjusting the position of the magnetic core, the variation of the peak and the Q value is very small by changing the turn number of the transformer coil. The results show that the broad tuning of the resonant frequency should be obtained by changing the turn number of the transformer coil, and the fine tuning should be achieved by adjusting the position of the magnetic core in order that the high Q value can be kept.

Noise power measurement of different laser power P without modulation is shown in Fig. 7. When the input laser power is 90 μW, the noise power is 3 dB higher than electronic noise power at the resonance frequency (test in 34.5 MHz). So the noise equivalent laser power is about 90 μW, and the corresponding DC photocurrent is 67.5 μA ($I_p = P\eta$, η is the responsivity of the photodiode ETX500T, which is about 0.75 A/W at 1064 nm), which is reasonably consistent with the calculated noise equivalent photocurrent $I_{ne} = 62$ μA. The total input current noise density (It can be regarded as a noise source which is added to the photodiode) can be calculated $i_n = \sqrt{2eI_{ne}}$ = 4.7 pA/$\sqrt{\text{Hz}}$. Besides, when the laser power is $2^{\alpha} - 1$ (α is equal to 1, 2, 3, 4, ... in turn) times that of noise equivalent laser power, the noise power has a regular increase of 3 dB. The noise power is proportional to the DC photocurrent and the laser power. Besides, the noise equivalent photocurrent is constant for a given circuit. So the noise power follows the same rules with the ratio between the DC photocurrent and the noise equivalent photocurrent. The resonant circuit effectively suppresses the noise at other frequencies which is away from the resonance frequency. The noise equivalent power can be lower at wavelengths where the photodiode has higher responsivity or if a new operational amplifier with lower input current noise adopted.

IV. CONCLUSION

The transformer-coupled LC resonant circuit has unique advantages in the photodetector design. It is benefit of increasing the gain of the photodetector and reducing the electronic noise of the photodetector. As a result, we obtain a low-noise, high gain photodetector with the gain of more than 1.8 $\times 10^5$ V/A and the input current noise of less than 4.7 pA/$\sqrt{\text{Hz}}$. By adjusting the parameter of the transformer, the quality factor Q of the resonant circuit is close to 100 over a frequency range of more than 100 MHz, which meets the requirement for weak power detection in the application of squeezed state generation. By choosing the operational amplifier with lower input current noise, we wish that a lower noise photodetector can be obtained.

ACKNOWLEDGMENTS

The work is supported by National Natural Science Foundation of China (Grant Nos. 61575114 and 11654002), in part by the National Key Research and Development Program of China (No. 2016YFA0301401), the Program for Sanjin Scholar of Shanxi Province, and the program for Outstanding Innovative Teams of Higher Learning Institutions of Shanxi.

[1] K. Goda, O. Miyakawa, E. E. Mikhailov, S. Saraf, R. Adhikari, K. McKenzie, R. Ward, S. Vass, A. J. Weinstein, and N. Mavalvala, Nat. Phys. **4**(6), 472–476 (2008).
[2] H. Grote, K. Danzmann, K. L. Dooley, R. Schnabel, J. Slutsky, and H. Vahlbruch, Phys. Rev. Lett. **110**, 181101 (2013).
[3] S. L. Braunstein and P. van Loock, Rev. Mod. Phys. **77**, 513 (2005).
[4] A. Furusawa, J. L. Sorensen, S. L. Braunstein, C. A. Fuchs, J. J. Kimble, and E. S. Polzik, Science **282**, 706 (1998).
[5] H. Vahlbruch, M. Mehmet, S. Chelkowski, and R. Schnable, Phys. Rev. Lett. **100**, 033602 (2008).
[6] T. Eberle, S. Steinlechner, J. Bauchrowitz, V. Haendchen, H. Vahlbruch, M. Mehmet, H. Ebhardt, and R. Schnabel, Phys. Rev. Lett. **104**, 251102 (2010).
[7] H. Vahlbruch, M. Mehmet, K. Danzmann, and R. Schnabel, Phys. Rev. Lett. **117**(11), 110801 (2016).

[8]R. W. P. Drever, J. L. Hall, F. V. Kowalski, J. Hough, G. M. Ford, A. J. Munley, and H. Ward, Appl. Phys. B **31**, 97 (1983).
[9]E. D. Black, Am. J. Phys. **69**, 79 (2001).
[10]S. Dwyer, L. Barsotti, S. S. Y. Chua, M. Evans, M. Factourovich, D. Gustafson, T. Isogai, K. Kawabe, A. Khalaidovski, P. K. Lam, M. Landry, N. Mavalvala, D. E. McClelland, G. D. Meadors, C. M. Mow-Lowry, R. Schnabel, R. M. S. Schofield, N. Smith-Lefebvre, M. Stefszky, C. Vorvick, and D. Sigg, Opt. Express **21**(16), 19047 (2013).
[11]Z. Li, W. Ma, W. Yang, Y. Wang, and Y. Zheng, Opt. Lett. **41**(14), 3331–3334 (2016).
[12]T. Eberle, V. Händchen, and R. Schnabel, Opt. Express **21**(9), 11546 (2013).
[13]Y. Zhou, X. Jia, F. Li, C. Xie, and K. Peng, Opt. Express **23**(4), 4952 (2015).
[14]M. Mehmet, S. Ast, T. Eberle, S. Steinlechner, H. Vahlbruch, and R. Schnabel, Opt. Express **19**(25), 25763 (2011).
[15]S. Bickman and D. DeMille, Rev. Sci. Instrum. **76**(11), 113101 (2005).
[16]H. Zhou, W. Yang, Z. Li, X. Li, and Y. Zheng, Rev. Sci. Instrum. **85**(1), 013111 (2014).
[17]S. Wang, X. Xiang, C. Zhou, Y. Zhai, R. Quan, M. Wang, F. Hou, S. Zhang, R. Dong, and T. Liu, Rev. Sci. Instrum. **88**(1), 013107 (2017).
[18]N. A. Lockerbie and K. V. Tokmakov, Rev. Sci. Instrum. **85**(11), 114705 (2014).
[19]N. Mio, M. Ando, G. Heinzel, and S. Moriwaki, Jpn. J. Appl. Phys., Part 1 **40**(1R), 426 (2001).
[20]H. Grote, Rev. Sci. Instrum. **78**(5), 054704 (2007).
[21]T. E. Darcie, B. L. Kaspar, and J. R. Talman, J. Lightwave Technol. **6**(4), 582 (1988).
[22]C. Chen, Z. Li, X. Jin, and Y. Zheng, Rev. Sci. Instrum. **87**(10), 103114 (2016).
[23]S. Potnis and A. C. Vutha, Rev. Sci. Instrum. **87**(7), 076104 (2016).
[24]C. K. Alexander and M. N. O. Sadiku, *Fundamentals of Electric Circuits* (McGraw-Hill, Boston, 2000).
[25]C. Bowick, *RF Circuit Design* (Newnes, 2011).
[26]G. Heinzel, *Advanced Optical Techniques for Laser-Interferometric Gravitational-Wave Detectors* (MPQ, 1999), Vol. 243.